Int j simul model 23 (2024) 4, 563-574
Original scientific paper

# OPTIMIZATION OF CONTAINER TERMINAL OPERATIONS USING RESPONSE SURFACE METHODOLOGY

Tuncel, G.* & Deniz, E.**
* Dokuz Eylul University, Department of Industrial Engineering, Izmir, Turkey
** Dokuz Eylul University, Graduate School of Natural and Applied Sciences, Izmir, Turkey
E-Mail: gonca.tuncel@deu.edu.tr, elvandeniz@comu.edu.tr

**Abstract**
Container terminals are essential for handling the growing container traffic resulting from global trade. Operation managers must either increase the number of handling components or improve the efficiency of existing equipment to meet the increasing demand. This paper employs the response surface methodology to obtain the optimal number of yard trucks (YTs) and rubber tyred gantry (RTG) cranes. First, a two-level full factorial design was employed to fit first-order regression models and assess the effects of the variables. Then, the second-order models were constructed with a central composite design to further explore the influence of key parameters on the response variables. The Derringer-Suich method was applied to identify the optimal levels of performance criteria such as operation time and cost. According to the implementation results, the average operation time was reduced from 303.25 minutes to 286.25 minutes, reflecting a 5.6 % improvement in operational efficiency. Furthermore, the total operating costs decreased by $315.72, from $2,331.59 to $2,015.87. This 13.5 % improvement highlights the operational cost advantages achieved by optimizing resources.
(Received in June 2024, accepted in October 2024. This paper was with the authors 5 weeks for 2 revisions.)

**Keywords:** Container Terminal, Double Cycling, Simulation, Response Surface Methodology, Derringer-Suich Method

## 1. INTRODUCTION

Marine container terminals play a critical role in global supply chains, acting as gateways that enable goods to flow between international shipping routes and inland distribution networks. With the increase of container volumes in recent years, improving the operational efficiency of handling components has become even more important to minimize delays and ensure the efficient movement of goods through the supply chain [1]. Possible disruptions in any of the logistics processes in a port (e.g., the inefficient operation of yard trucks or cranes) will affect the speed of container handling and increase the waiting times of vessels at the quay. Vessels waiting at the quay will prevent cargo owners from receiving their cargo at the scheduled time and will cause financial losses to the carrier by increasing container terminal costs. Most container terminals have three types of handling equipment: quay crane (QC), rubber tyred gantry (RTG) crane, and yard truck (YT). Quay cranes are essential equipment for container terminals. Therefore, planning QC operations is a crucial factor that significantly affects the operational effectiveness of maritime container terminals [2]. Two operating strategies are employed in planning the QC function: single and double cycling. The operating strategy in which the QCs carry out the handling operations after completing the unloading of all containers in the vessel bay is defined as single cycling. Double cycling is a terminal operating technique in which QCs simultaneously perform loading and unloading tasks within the same vessel bay. A QC starts the container handling process from the relevant bay and loads the related containers onto the YTs, which transport them to the stockyard. The RTG then unloads containers from the YTs and stacks them in designated blocks. The released YTs are directed to the nearest stockyard where the next set of containers will be loaded.

Goodchild and Daganzo [3] first introduced the double cycling strategy for QCs to minimize vessel turnaround time in container terminals. In the next study, the authors demonstrated how this technique significantly improves operational efficiency [4]. Zhang and Kim [5] expanded the problem to include multiple hatches. The authors developed a mixed integer programming (MIP) model and employed a hybrid heuristic method to resolve the problem. Nguyen and Kim [6] proposed a modified MIP model and a heuristic algorithm to minimize empty trips of YTs by the QC double cycling method. A simulation technique was developed to evaluate the effect of unloading and loading schedules, and storage plans for unloaded containers on system efficiency. Lee et al. [7] considered a more complex scenario including hatch covers. In the same year, Zhang et al. [8] formulated a MIP model for the double cycling process described as a three-stage hybrid flow shop problem with no-buffer and multi-job families. The quay crane double cycling problem (QCDCP) was also investigated by Wang and Li [9]. The problem is presented as a two-machine non-permutation flow-shop scheduling model, and a composite heuristic for solving it is described. Zeng et al. [10] proposed a scheduling model and designed algorithms for the QCDCP. A MIP model was formulated to develop a stacking plan for outbound containers and the process order of QCs to increase the performance progress of the QCDC. The integrated double cycling problem of QCs and YCs was considered by Zhang et al. [11]. The aim was to minimize the processing time of QC and YC. They developed a MIP model for the two-stage double cycling process of container terminals. Numerical results showed that the specified model and algorithm were more efficient compared to the lower bounds presented in previous studies. Ku and Arthanari [12] considered the multi-QC double cycling problem. A two-stage hybrid heuristic approach was presented to solve the scheduling problem in numerous hatches. Chu et al. [13] formulated a mathematical model for the "multiple-QC sequencing problem" with the strategy of double cycling. The authors proposed an algorithm based on Lagrange relaxation to solve the model. Zhang et al. [14] analysed the performance of double cycling operations based on different equipment variations using the data from Tianjin Port in China. In the same year, Kamble et al. [15] explored the obstacles to implementing a double cycling strategy in Indian ports. The authors concluded that the main obstacle to implementation is the capability to use information technologies in ports and integrate with other ports and partners. Tang et al. [16] presented an agent-based simulation model to define QCs, YCs, and YT operation processes. Deniz et al. [17] developed simulation models to analyse the effects of the multi-QC single and double cycling strategies on the overall system performance. Ahmed et al. [18] implemented a container handling strategy using double cycling of YTs to minimize unit cost. They presented simulation models based on a case study, considering uncertainties in task durations. Fontes and Homayouni [19] considered the joint scheduling problem of QCs and speed-adjustable automated guided vehicles (AGVs) under the double cycling strategy. The authors address the energy consumption of seaports. Cai et al. [20] proposed a MIP model for the integrated scheduling of QCs, YCs, and intelligent guided vehicles in a U-shaped container terminal that applies a double cycling strategy. Tan et al. [21] investigated the storage space allocation problem in a container yard under the double-cycle operation mode for internal YTs. Li et al. [22] considered the multiple-equipment integrated scheduling problem in automated container terminals to optimize container work sequences.

Double cycling in container terminals is a rather new topic. In the literature, real-world systems that require practical extensions to be considered simultaneously have not been adequately handled. On the other hand, the existing methodologies for optimizing container handling operations under different operating strategies mostly rely on mathematical programming techniques. These approaches focus on developing analytical and algorithmic solutions for highly constrained problems. Mathematical models are built on certain assumptions and simplifications to reduce the complexity of real-world scenarios. However, in complex environments such as container handling, oversimplification can compromise the accuracy and usefulness of the model. The relationships between input variables and the system's outputs (e.g., operation time, cost, or efficiency) are highly non-linear and intricate, making it difficult to account for these dependencies in a single global function. Simulation-based optimization is a more flexible, integrated, and adaptive approach to handle the dynamic and uncertain nature of container handling. This study considers a real-world port where the handling process is conducted using multi-QC single and double cycling strategies. The main contribution is to propose a simulation-based optimization approach using response surface methodology (RSM) to increase efficiency and reduce costs associated with container loading and unloading operations. We extended the simulation models presented by Deniz et al. [17] by integrating an optimization procedure to minimize the average operation time and total operating cost. The optimal settings of system parameters were determined using RSM to minimize the performance criteria. A central composite design (CCD) in the form of a $2^5$ full factorial design was used for fitting second-order regression models.

The paper is organized as follows: In Section 2, a case study is introduced to illustrate RSM. The optimization process and the results of the implementation study are presented in Section 3. Finally, the summary and concluding remarks are given in Section 4.

## 2. PROBLEM DEFINITION

The proposed methodology aims to improve container handling operations, minimize vessel turnaround times, and ultimately minimize handling costs at the container terminal. We developed the simulation models using Arena simulation software for two scenarios: the multi-QC single cycling model and the multi-QC double and single cycling model. For this purpose, the handling process of 40-foot containers, which is carried out using three QCs from three separate bays in the container terminal, is addressed with two different modelling approaches. The multi-QC single cycling strategy was used in the first model, while the multi-QC double and single cycling strategy was used in the second model. The simulation models have a structure that can be easily adapted to varying conditions by adjusting the system parameters such as the number of QCs, RTGs, and YTs (for further reading on the simulation models, see Deniz et al. [17]). After fitting the first-order regression models to the data, we constructed the CCD for the estimation of curvature in the response surface. We then applied the Derringer-Suich method to optimize multiple responses simultaneously. The response optimization tool of Minitab software was used to estimate the optimal level of each variable. The proposed approach is illustrated through a case study conducted in Ambarlı Port, Turkey. We applied the RSM procedure to create a metamodel (a response surface) based on simulation experiments in a two-stage manner. The first stage of the RSM starts once the main independent variables have been identified through a screening experiment. The goal is to determine whether the current levels of the independent variables result in a near-optimal response value or whether the process is operating in another region far from the optimum values [23, 24]. Five input factors related to vessel operations were identified to minimize unloading and loading times as well as operating costs.

The following independent variables are used in the formulation:

- ***T*:** number of YTs in the system,
- ***E*:** number of RTGs in the E-Import stockyard,
- ***F*:** number of RTGs in the F-Export stockyard,
- ***G*:** number of RTGs in the G-Export stockyard,
- ***H*:** number of RTGs in the H-Import stockyard.

The following response variables are used in the formulation:

- **$Y_1$:** average operation time,
- **$Y_2$:** total cost including depreciation ($),

- $\boldsymbol{Y_3}$**:** total operating cost ($).

First, it was determined whether the levels of the independent variables in the region of interest yielded results close to the optimum point in the system's response. The curvature in the generated response surface becomes more obvious as it approaches the optimum point. The input factors were analysed for both high and low levels using the one-factor-at-a-time (OFAT) method. Then, the effect of a change in one factor was analysed based on the output when all other factors were constant [23]. The OFAT approach was used to evaluate the effect of YTs on the operation time. Since there are 3 QCs in the system, there must be a minimum of 3 YT assignments. According to the interviews held at the port, a maximum of 24 YT can be assigned to 3 QCs in the container terminal. There are 4 stockyards in this system, with 2 RTGs kept constant in each stockyard. The system was simulated for 3, 6, 9, and 10 YTs, and a total of 18 simulation experiments were conducted by increasing the number of YTs by 1 until reaching 24 YTs. Average operation times obtained from the simulation experiments were graphically illustrated in Fig. 1 a. The graphic trend declines after the 12$^{th}$ YT and continues similarly until the 24$^{th}$ YT. A similar situation is also observed in Fig. 1 b. Hence, the OFAT ranges for the YT were determined as 12–24.

Furthermore, we defined the ranges by setting the lower and upper limits (-1, +1) and selecting intermediate values (-0.5, 0, +0.5) for the second stage of the RSM. For instance, if we set the lower and upper limits as 11–24, the number of YTs for the intermediate points (–0.5, 0, +0.5 values) would be 14.25, 17.5, and 20.75. Similarly, if we set the lower and upper limits as 13–24, the number of YTs for the intermediate points (–0.5, 0, +0.5 values) would be 15.75, 18.5, and 21.25. On the other hand, the number of YTs must be integers in simulation. When selecting the range, the lower limit was set to 16 and the upper limit to 24, ensuring that the number of YT at the intermediate points is always an integer. In these ranges, the numbers of YTs for intermediate values (–0.5, 0, +0.5) would be 18, 20, and 22, respectively. However, the numbers of YTs before 16 were not included in the RSM, as they may prevent us from reaching the optimum point (see Fig. 1).

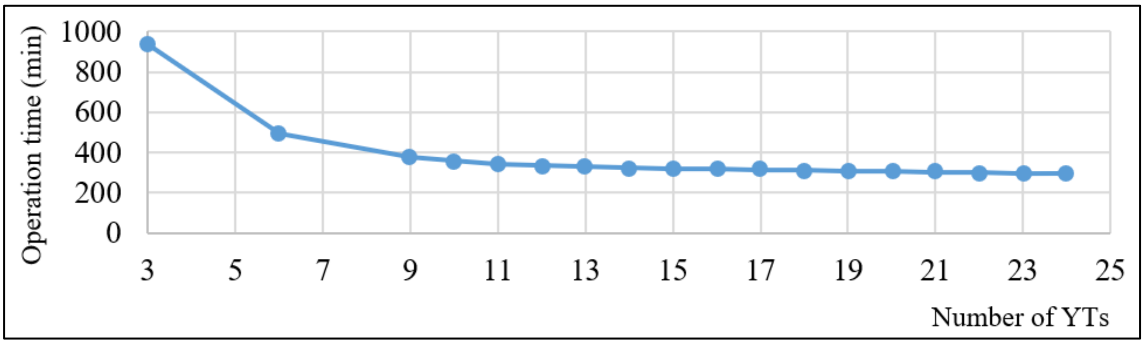


a) Number of YTs from 3 to 24

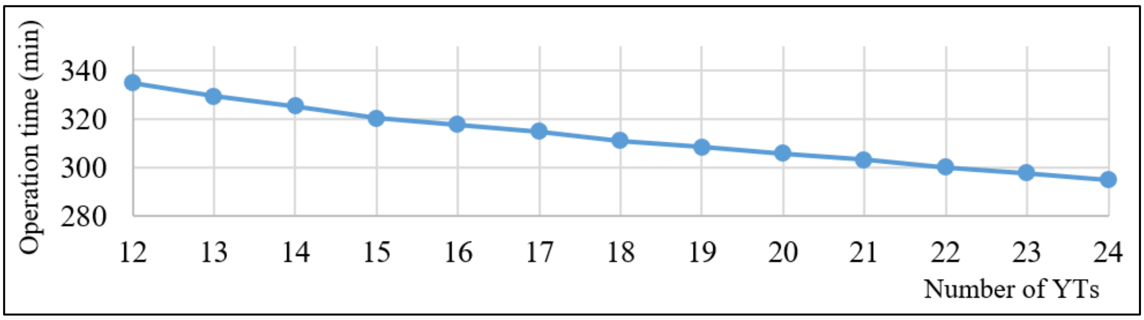


b) Number of YTs from 12 to 24

Figure 1: Effect of YTs on operation time using the OFAT approach.

The OFAT method was used to evaluate the effect of RTGs on the response. There are 8 stockyards and 41 RTGs in the port. A maximum of 8 RTGs can operate in each stockyard. OFAT was applied by systematically changing the number of RTGs in each experiment. First, the number of YTs was held constant at 21. Then, the simulation model was run by varying the number of RTGs in a stockyard between 1 and 8, while keeping the number of RTGs in other stockyards constant at 2. When we consider applying the OFAT approach for the E-Import stockyard, there will be two RTGs in the other stockyards, and the number of YTs will remain constant at 21. The number of RTGs in the E-Import stockyard is adjusted sequentially from 1 to 8, and a simulation is conducted for each configuration. The average operation times obtained from the simulation experiments are presented in Fig. 2.

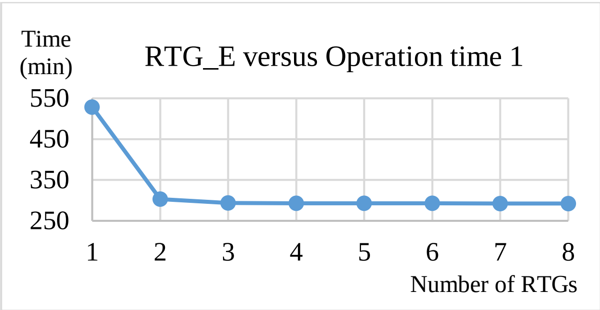


a) RTG_E from 1 to 8

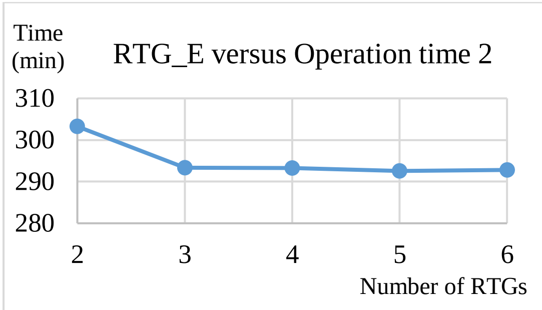


b) RTG_E from 2 to 6

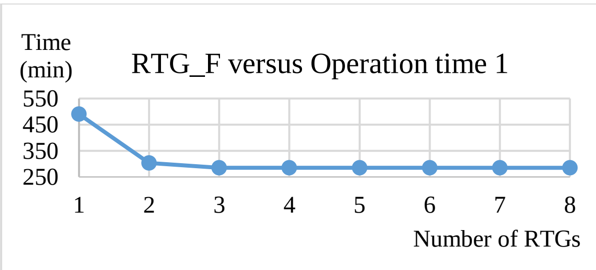


c) RTG_F from 1 to 8

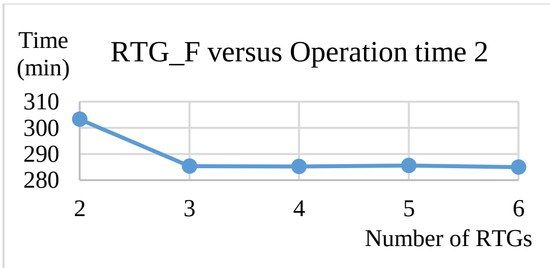


d) RTG_F is from 2 to 6

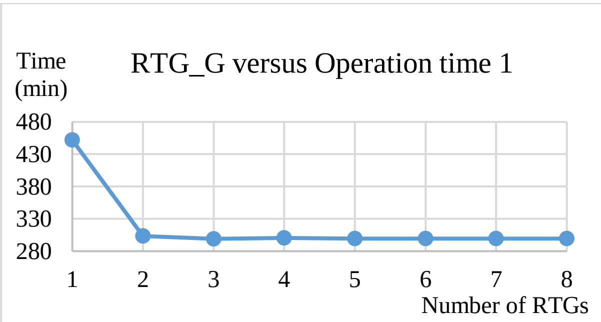


e) RTG_G from 1 to 8

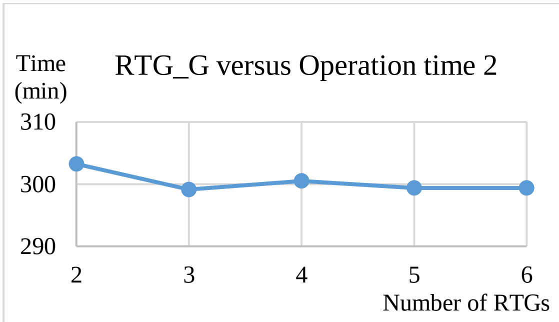


f) RTG_G from 2 to 6

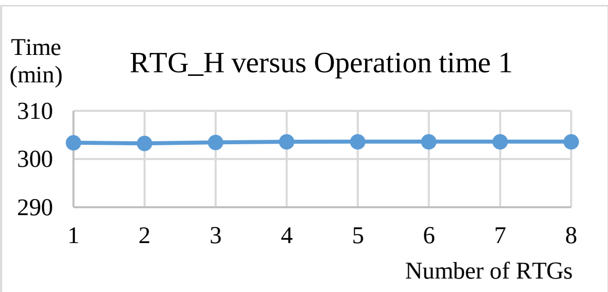


g) RTG_H from 1 to 8

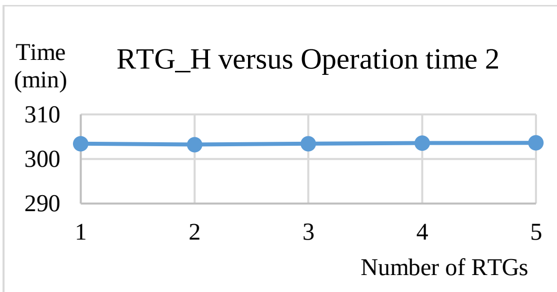


h) RTG_H from 1 to 5

Figure 2: Effect of RTGs on operation time using the OFAT approach.

When analysing Fig. 2 a, c, and e, the graphical trend shows a significant decrease after the 2nd RTG and remains relatively stable until the 8th RTG. As seen in Fig. 2 g, there is no significant difference between the first and the 8th RTGs. A similar situation is observed in Fig. 2 b, d, f, and h. OFAT ranges of the RTGs were determined as 1–5 for the H-Import stockyard and 2–6 for the other stockyards. Table I shows the three levels of independent variables (low, central, and high) determined by the OFAT study. The coded values at three levels are calculated by transforming the natural variables.

Table I: Independent variables and their coded levels for the central composite design.

| Levels of coded variables | Independent variables | | | | |
|---|---|---|---|---|---|
| | **YT (*T*)** | **RTG_E (*E*)** | **RTG_F (*F*)** | **RTG_G (*G*)** | **RTG_H (*H*)** |
| Low (-1) | 12 | 2 | 2 | 2 | 1 |
| Medium (0) | 18 | 4 | 4 | 4 | 3 |
| High (1) | 24 | 6 | 6 | 6 | 5 |

The first-order regression models with two-factor interactions are assumed to be:

$$Y_1 = \alpha_0 + \alpha_1 T + \alpha_2 E + \alpha_3 F + \alpha_4 G + \alpha_5 H + \alpha_{12} TE + \alpha_{13} TF + \alpha_{14} TG + \alpha_{15} TH + \alpha_{23} EF + \alpha_{24} EG + \alpha_{25} EH + \alpha_{34} FG + \alpha_{35} FH + \alpha_{45} GH + \varepsilon \quad (1)$$

$$Y_2 = \beta_0 + \beta_1 T + \beta_2 E + \beta_3 F + \beta_4 G + \beta_5 H + \beta_{12} TE + \beta_{13} TF + \beta_{14} TG + \beta_{15}^{TH} + \beta_{23} EF + \beta_{24} EG + \beta_{25} EH + \beta_{34} FG + \beta_{35} FH + \beta_{45} GH + \varepsilon \quad (2)$$

$$Y_3 = \delta_0 + \delta_1 T + \delta_2 E + \delta_3 F + \delta_4 G + \delta_5 H + \delta_{12} TE + \delta_{13} TF + \delta_{14} TG + \delta_{15}^{TH} + \delta_{23} EF + \delta_{24} EG + \delta_{25} EH + \delta_{34} FG + \delta_{35} FH + \delta_{45} GH + \varepsilon \quad (3)$$

## 3. RESPONSE SURFACE METHODOLOGY

The two-level full factorial design ($2^5$) was conducted with central runs, and the simulation model was run for ten independent replications at each design point. Thus, response values were determined for each design point. We find the coefficient estimation values that will minimize the residuals by the least squares technique. The following equations represent the first-order models fitting responses $Y_1$, $Y_2$, and $Y_3$:

$$Y_1 = 301.268 - 19.637\,T - 6.496\,E - 7.802\,F - 0.979\,G - 0.665\,H + 0.538\,TE + 1.068\,TF + 0.306\,TG + 0.538\,TH - 1.223\,EF + 0.007\,EG + 0.044\,EH + 0.079\,FG + 0.164\,FH - 0.002\,GH \quad (4)$$

$$Y_2 = 6302.23 + 100.63\,T + 243.60\,E + 217.13\,F + 344.73\,G + 351.63\,H - 22.53\,TE - 14.90\,TF - 18.30\,TG - 15.42\,TH - 40.40\,EF - 9.13\,EG - 7.75\,EH - 8.01\,FG - 6.53\,FH - 2.72\,GH \quad (5)$$

$$Y_3 = 2270.27 + 276.24\,T + 15.64\,E + 6.39\,F + 41.27\,G + 43.75\,H - 7.81\,TE - 7.29\,TF - 1.95\,TG - 1.83\,TH - 8.85\,EF - 1.42\,EG - 0.62\,EH + 0.14\,FG + 0.45\,FH - 0.84\,GH \quad (6)$$

The analysis of variance (ANOVA) demonstrated that the main effects, two-way interactions, and curvature are statistically significant ($P$-value < 0.05). Moreover, the lack of fit is insignificant ($P$ > 0.05), implying the first-order regression models adequately described the data. In the second stage of the RSM, the second-order (quadratic) models were developed to capture the non-linear relationships between the independent variables and responses. The desirability function method was used to determine the optimal operating conditions that balance trade-offs between responses $Y_1$, $Y_2$, and $Y_3$ within the experimental region studied. The second-order regression models are as follows:

$$Y_1 = \alpha_0 + \alpha_1 T + \alpha_2 E + \alpha_3 F + \alpha_4 G + \alpha_5 H + \alpha_{11} T^2 + \alpha_{22} E^2 + \alpha_{33} F^2 + \alpha_{44} G^2 + \alpha_{55} H^2 + \alpha_{12} TE + \alpha_{13} TF + \alpha_{14} TG + \alpha_{15} TH + \alpha_{23} EF + \alpha_{24} EG + \alpha_{25} EH + \alpha_{34} FG + \alpha_{35} FH + \alpha_{45} GH + \varepsilon \quad (7)$$

$$Y_2 = \beta_0 + \beta_1 T + \beta_2 E + \beta_3 F + \beta_4 G + \beta_5 H + \beta_{11} T^2 + \beta_{22} E^2 + \beta_{33} F^2 + \beta_{44} G^2 + \beta_{55} H^2 + \beta_{12} TE + \beta_{13} TF + \beta_{14} TG + \beta_{15} TH + \beta_{23} EF + \beta_{24} EG + \beta_{25} EH + \beta_{34} FG + \beta_{35} FH + \beta_{45} GH + \varepsilon \quad (8)$$

$$Y_3 = \delta_0 + \delta_1 T + \delta_2 E + \delta_3 F + \delta_4 G + \delta_5 H + \delta_{11} T^2 + \delta_{22} E^2 + \delta_{33} F^2 + \delta_{44} G^2 + \delta_{55} H^2 + \delta_{12} TE + \delta_{13} TF + \delta_{14} TG + \delta_{15} TH + \delta_{23} EF + \delta_{24} EG + \delta_{25} EH + \delta_{34} FG + \delta_{35} FH + \delta_{45} GH + \varepsilon \quad (9)$$

A central composite design (CCD), one of the most commonly used experimental designs for fitting second-order models in RSM, was utilized with three levels for each of the five variables. A CCD is created by increasing the two-level full factorial design with centre and axial runs ($\alpha = 1$ indicates a face-centred design) to fit second-order models. The two-level full factorial design points and the values for axial points represent the averages of ten replications. Second-order regression models derived from the CCD for $Y_1$, $Y_2$, and $Y_3$ are as follows:

$$Y_1 = 279.833 - 19.445\,T - 6.409\,E - 7.901\,F - 0.941\,G - 0.649\,H + 4.577\,TT + 5.642\,EE + 9.672\,FF + 0.577\,GG + 0.952\,HH + 0.538\,TE + 1.068\,TF + 0.306\,TG + 0.538\,TH - 1.223\,EF + 0.007\,EG + 0.044\,EH + 0.079\,FG + 0.164\,FH - 0.002\,GH \quad (10)$$

$$Y_2 = 5957.164 + 102.522\,T + 244.260\,E + 214.275\,F + 343.853\,G + 350.373\,H + 56.177\,TT + 91.063\,EE + 169.456\,FF + 12.631\,GG + 15.405\,HH - 22.530\,TE - 14.902\,TF - 18.301\,TG - 15.424\,TH - 40.404\,EF - 9.127\,EG - 7.754\,EH - 8.012\,FG - 6.529\,FH - 2.721\,GH \quad (11)$$

$$Y_3 = 2191.163 + 275.992\,T + 16.054\,E + 5.572\,F + 41.197\,G + 43.581\,H - 0.371\,TT + 20.767\,EE + 49.622\,FF + 5.587\,GG + 3.372\,HH - 7.807\,TE - 7.286\,TF - 1.949\,TG - 1.830\,TH - 8.849\,EF - 1.422\,EG - 0.618\,EH + 0.140\,FG + 0.446\,FH - 0.837\,GH \quad (12)$$

After constructing regression models for the three responses, we verified and validated them. The lack-of-fit values for responses $Y_1$, $Y_2$, and $Y_3$ are 0.802, 0.820, and 0.849, respectively, indicating an insignificant lack-of-fit ($P > 0.05$). In addition, for response $Y_1$, the $R^2$ value is 99.63 %, the $R^2$-adjusted value is 99.41 %, and the $R^2$-predicted value is 99.06 %. For response $Y_2$, the $R^2$ value is 99.80 %, the $R^2$-adjusted value is 99.69 %, and the $R^2$-predicted value is 99.51 %. For response $Y_3$, the $R^2$ value is 99.93 %, the $R^2$-adjusted value is 99.88 %, and the $R^2$-predicted value is 99.88 %. Statistical checks indicated that the regression models provide an adequate approximation to the real system. For the validation, 32 random points within the experimental area that are different from the points used in the CCD were selected. The simulation model was run to generate the response values at the 32 randomly selected points using Arena simulation software. Metamodel values are the predictions for the three responses made by substituting the coded values into the respective regression equations. Absolute Relative Error (*ARE*) was used as a validation criterion to assess the accuracy of the predictive models. The *ARE* value is represented by *r*, the simulation output by *sy*, and the metamodel output by *my*. The *ARE* values of 32 points to be validated are obtained by using the following formula:

$$r = |(sy - my)/sy| \quad (13)$$

We observed that all *ARE* values for responses $Y_1$, $Y_2$, and $Y_3$ are less than 5 %. We hence conclude that second-order models yield good predictions of the system responses.

### 3.1 Multi-response optimization

The Derringer-Suich method uses a desirability function in which the importance levels (priorities) regarding response values are incorporated into a single optimization procedure. Initially, the target values of each response should be determined to define desirability functions. We aimed to reduce the total cost including depreciation to below $5,285 and the total operating cost to less than $2,275 while remaining below the average operation time of 303.25 minutes. Then, the *t* and *s* weight values were established. The values for *t* and *s* were used as 0.1, 1, and 10. With the combination of weights, 27 different conditions arise. Table II presents the weights of the responses, the combined desirability values, and the coded values of the independent variables that yield these desirability values. The coded values of the *T*, *E*, *F*, *G*, and *H* input factors in Table II were converted into real (natural) values by considering the low (-1) and high (1) levels of independent variables presented in Table I. Since the optimum levels of input factors are determined using the metamodel, confirmatory simulation studies are also required at these input levels.

Table II: Composite desirability and coded values with corresponding weights.

| | **Weights** | | | **Composite desirability** | **Independent variables in coded form** | | | | |
|---|---|---|---|---|---|---|---|---|---|
| | $Y_1$ | $Y_2$ | $Y_3$ | | ***T*** | ***E*** | ***F*** | ***G*** | ***H*** |
| 1 | 0.1 | 0.1 | 0.1 | 0.974377 | -0.353535 | -0.030300 | 0.070707 | -1 | -1 |
| 2 | 0.1 | 0.1 | 1 | 0.969737 | -0.959596 | 0.191919 | 0.151515 | -1 | -1 |
| 3 | 0.1 | 0.1 | 10 | 0.969253 | -0.979798 | 0.212121 | 0.232323 | -1 | -1 |
| 4 | 0.1 | 1 | 0.1 | 0.952625 | -0.494949 | -0.838384 | -0.393939 | -1 | -1 |
| 5 | 0.1 | 1 | 1 | 0.947932 | -0.898990 | -0.696970 | -0.292929 | -1 | -1 |
| 6 | 0.1 | 1 | 10 | 0.947918 | -0.898990 | -0.717172 | -0.272727 | -1 | -1 |
| 7 | 0.1 | 10 | 0.1 | 0.909920 | -0.916586 | -1 | -0.676768 | -1 | -1 |
| 8 | 0.1 | 10 | 1 | 0.909689 | -0.939394 | -1 | -0.656566 | -1 | -1 |
| 9 | 0.1 | 10 | 10 | 0.909491 | -0.939394 | -1 | -0.636364 | -1 | -1 |
| 10 | 1 | 0.1 | 0.1 | 0.955243 | 0.959596 | 0.050505 | -0.030300 | -1 | -1 |
| 11 | 1 | 0.1 | 1 | 0.817156 | -0.333333 | 0.313131 | 0.272727 | -1 | -1 |
| 12 | 1 | 0.1 | 10 | 0.775677 | -0.965810 | 0.070707 | 0.311293 | -1 | -1 |
| 13 | 1 | 1 | 0.1 | 0.885466 | 0.777778 | -0.131313 | -0.010100 | -1 | -1 |
| 14 | 1 | 1 | 1 | 0.771382 | -0.353535 | -0.030300 | 0.070707 | -1 | -1 |
| 15 | 1 | 1 | 10 | 0.736127 | -0.944505 | -0.030300 | 0.212121 | -1 | -1 |
| 16 | 1 | 10 | 0.1 | 0.660600 | -0.171717 | -0.919192 | -0.454545 | -1 | -1 |
| 17 | 1 | 10 | 1 | 0.615488 | -0.494949 | -0.838384 | -0.393939 | -1 | -1 |
| 18 | 1 | 10 | 10 | 0.585830 | -0.898990 | -0.696970 | -0.292929 | -1 | -1 |
| 19 | 10 | 0.1 | 0.1 | 0.951940 | 1 | -0.191919 | 0.090909 | -1 | -0.757576 |
| 20 | 10 | 0.1 | 1 | 0.677229 | 0.997268 | -0.131313 | 0.090909 | -1 | -1 |
| 21 | 10 | 0.1 | 10 | 0.142767 | -0.353535 | 0.373737 | 0.313131 | -1 | -1 |
| 22 | 10 | 1 | 0.1 | 0.881239 | 1 | 0.030303 | -0.070700 | -1 | -1 |
| 23 | 10 | 1 | 1 | 0.623892 | 1 | -0.171717 | 0.151515 | -1 | -1 |
| 24 | 10 | 1 | 10 | 0.132755 | -0.333333 | 0.313131 | 0.272727 | -1 | -1 |
| 25 | 10 | 10 | 0.1 | 0.405700 | 1 | -0.151515 | -0.030300 | -1 | -1 |
| 26 | 10 | 10 | 1 | 0.296290 | 0.777778 | -0.131313 | -0.010100 | -1 | -1 |
| 27 | 10 | 10 | 10 | 0.074593 | -0.353535 | -0.030300 | 0.070707 | -1 | -1 |

Table III presents the results of confirmatory experiments conducted using the Derringer-Suich multi-response optimization method, based on weight combinations and confirmatory simulation outcomes. The last row of the table shows the initial parameter setting and validated simulation results. The upper limits for the responses were set at 303.25 minutes ($Y_1$), \$5,285 ($Y_2$), and \$2,275 ($Y_3$). The goal was to minimize these values within the constraints. Implementation results reveal the combinations of weights that successfully meet the target levels for all three responses. It can be seen that three values meet the target level of response $Y_1$. The first value is 300.07 minutes presented in rows 5, 6, and 18. The second one yields a result of 295.30 minutes in row 16. Finally, the third value of 286.25 minutes is achieved in rows 1, 14, and 27. The lowest value of the average operation time is highlighted in grey rows in Table III. We thus conclude that response $Y_1$ was optimized to 286.25 minutes, response $Y_2$ to \$5,239.5, and response $Y_3$ to \$2,015.9. These three responses are achieved using the optimal configuration of 16 YTs, 4 RTG_Es, 4 RTG_Fs, 2 RTG_Gs, and 1 RTG_H.

Table III: Results of confirmatory experiments.

| | **Weights** | | | **Composite desirability** | **Natural variables** | | | | | **Metamodel results** | | | **Simulation results** | | |
|---|---|---|---|---|---|---|---|---|---|---|---|---|---|---|---|
| | $Y_1$ | $Y_2$ | $Y_3$ | | $T$ | $E$ | $F$ | $G$ | $H$ | $Y_1$ | $Y_2$ | $Y_3$ | $Y_1$ | $Y_2$ | $Y_3$ |
| 1* | 0.1 | 0.1 | 0.1 | 0.974377 | 16 | 4 | 4 | 2 | 1 | 290.35 | 5256.5 | 2015.7 | 286.25 | 5239.5 | 2015.9 |
| 2 | 0.1 | 0.1 | 1 | 0.969737 | 12 | 4 | 4 | 2 | 1 | 304.30 | 5306.4 | 1854.1 | 306.86 | 5244.6 | 1847.3 |
| 3 | 0.1 | 0.1 | 10 | 0.969253 | 12 | 4 | 4 | 2 | 1 | 304.32 | 5336.6 | 1851.5 | 306.86 | 5244.6 | 1847.3 |
| 4 | 0.1 | 1 | 0.1 | 0.952625 | 15 | 2 | 3 | 2 | 1 | 308.23 | 4990.2 | 1973.5 | 303.89 | 4885.4 | 1956.5 |
| 5 | 0.1 | 1 | 1 | 0.947932 | 13 | 3 | 3 | 2 | 1 | 315.71 | 4994.6 | 1854.4 | 300.07 | 4861.1 | 1839.9 |
| 6 | 0.1 | 1 | 10 | 0.947918 | 13 | 3 | 3 | 2 | 1 | 315.73 | 4994.8 | 1854.2 | 300.07 | 4861.1 | 1839.9 |
| 7 | 0.1 | 10 | 0.1 | 0.90992 | 13 | 2 | 3 | 2 | 1 | 327.76 | 4906.0 | 1862.1 | 316.90 | 4898.7 | 1874.5 |
| 8 | 0.1 | 10 | 1 | 0.909689 | 12 | 2 | 3 | 2 | 1 | 328.03 | 4905.7 | 1854.5 | 324.23 | 4917.2 | 1838.5 |
| 9 | 0.1 | 10 | 10 | 0.909491 | 12 | 2 | 3 | 2 | 1 | 327.61 | 4907.0 | 1853.6 | 324.23 | 4917.2 | 1838.5 |
| 10 | 1 | 0.1 | 0.1 | 0.955243 | 24 | 4 | 4 | 2 | 1 | 267.64 | 5476.8 | 2383.3 | 270.56 | 5547.0 | 2397.0 |
| 11 | 1 | 0.1 | 1 | 0.817156 | 16 | 5 | 5 | 2 | 1 | 286.99 | 5415.0 | 2034.7 | 285.69 | 5574.1 | 2056.8 |
| 12 | 1 | 0.1 | 10 | 0.775677 | 12 | 4 | 5 | 2 | 1 | 304.40 | 5320.8 | 1854.2 | 306.79 | 5426.7 | 1869.1 |
| 13 | 1 | 1 | 0.1 | 0.885466 | 23 | 4 | 4 | 2 | 1 | 270.90 | 5395.6 | 2330.7 | 271.23 | 5487.8 | 2342.9 |
| 14* | 1 | 1 | 1 | 0.771382 | 16 | 4 | 4 | 2 | 1 | 290.35 | 5256.5 | 2015.7 | 286.25 | 5239.5 | 2015.9 |
| 15 | 1 | 1 | 10 | 0.736127 | 12 | 4 | 4 | 2 | 1 | 304.91 | 5260.6 | 1854.0 | 306.86 | 5244.6 | 1847.3 |
| 16 | 1 | 10 | 0.1 | 0.6606 | 17 | 2 | 3 | 2 | 1 | 302.63 | 5012.8 | 2069.9 | 295.30 | 4914.5 | 2040.2 |
| 17 | 1 | 10 | 1 | 0.615488 | 15 | 2 | 3 | 2 | 1 | 308.23 | 4990.2 | 1973.5 | 303.89 | 4885.4 | 1956.5 |
| 18 | 1 | 10 | 10 | 0.58583 | 13 | 3 | 3 | 2 | 1 | 315.71 | 4994.6 | 1854.4 | 300.07 | 4861.1 | 1839.9 |
| 19 | 10 | 0.1 | 0.1 | 0.95194 | 24 | 4 | 4 | 2 | 1 | 267.61 | 5535.3 | 2402.0 | 270.56 | 5547.0 | 2397.0 |
| 20 | 10 | 0.1 | 1 | 0.677229 | 24 | 4 | 4 | 2 | 1 | 267.59 | 5471.6 | 2392.5 | 270.56 | 5547.0 | 2397.0 |
| 21 | 10 | 0.1 | 10 | 0.142767 | 16 | 5 | 5 | 2 | 1 | 287.13 | 5445.6 | 2032.4 | 285.69 | 5574.1 | 2056.8 |
| 22 | 10 | 1 | 0.1 | 0.881239 | 24 | 4 | 4 | 2 | 1 | 267.61 | 5473.8 | 2394.7 | 270.56 | 5547.0 | 2397.0 |
| 23 | 10 | 1 | 1 | 0.623892 | 24 | 4 | 4 | 2 | 1 | 267.60 | 5479.7 | 2393.8 | 270.56 | 5547.0 | 2397.0 |
| 24 | 10 | 1 | 10 | 0.132755 | 16 | 5 | 5 | 2 | 1 | 286.99 | 5415.0 | 2034.7 | 285.69 | 5574.1 | 2056.8 |
| 25 | 10 | 10 | 0.1 | 0.4057 | 24 | 4 | 4 | 2 | 1 | 268.48 | 5440.1 | 2392.9 | 270.56 | 5547.0 | 2397.0 |
| 26 | 10 | 10 | 1 | 0.29629 | 23 | 4 | 4 | 2 | 1 | 270.90 | 5395.6 | 2330.7 | 271.23 | 5487.8 | 2342.9 |
| 27* | 10 | 10 | 10 | 0.0745925 | 16 | 4 | 4 | 2 | 1 | 290.35 | 5256.5 | 2015.7 | 286.25 | 5239.5 | 2015.9 |
| Current system | | | | | 2 | 2 | 2 | 2 | 2 | | | | 303.25 | 5348.9 | 2331.6 |

### 3.2 Results of the performance analysis

The experimental results show that the proposed optimization approach significantly increases productivity and cost efficiency in container terminal operations compared to the existing system. The performance comparison between the current system configuration and the optimization results from the RSM is summarized in Table IV. We can draw the following conclusions from the implementation results:

- The average operation time was reduced from 303.25 minutes to 286.25 minutes, yielding a 17-minute advantage and a 5.6 % improvement. This translates to quicker container handling and reduced vessel turnaround times.
- The total operating cost was reduced by $315.72 (from $2,331.59 to $2,015.87), showing a 13.5 % improvement. The total cost, including depreciation, decreased from $5,348.93 to $5,239.45, resulting in a savings of $109.48 and a 2.0 % improvement.
- The number of YTs decreased from 21 to 16, while the number of RTGs increased from 8 to 11, contributing to improved cost efficiency. This alternative will provide a cost advantage by reducing the total operating cost by $0.78 per container, and the total cost including depreciation the operating cost by $0.27.
- We note that the reduction of 5 YTs leads to significantly decreased internal traffic within the terminal, improving the flow of containers and reducing congestion. This not only improves operational efficiency but also minimizes fuel and maintenance costs for YTs.
- As an alternative scenario presented in rows 5, 6, and 18 of Table III, a response time of 300.07 minutes was achieved, providing a more modest reduction of 3.18 minutes, which equates to a 1.0 % improvement. While this improvement is smaller, it may be adequate for periods of lower workload, providing flexibility in resource allocation.
- If the alternative scenario is applied under lower workload conditions, the number of YTs decreases further, from 21 to 13, while the number of RTGs increases slightly, from 8 to 9. This adjustment significantly reduces internal traffic and overall costs, providing a more balanced approach when fewer resources are needed. The alternative scenario achieves a more substantial reduction in internal traffic by decreasing YTs to 13.

Table IV: Comparison of performance measures before and after optimization.

| Performance measures | Current system | RSM approach |
|---|---|---|
| Average operation time (min) | 303.25 | 286.25 |
| Total cost including depreciation ($) | 5,348.93 | 5,239.45 |
| Total operating cost ($) | 2,331.59 | 2,015.87 |

Implementing the optimized configuration provides significant benefits to operational efficiency and cost-effectiveness. By reducing the average operation time and adjusting the number of YTs and RTGs, the terminal can achieve better performance metrics such as vessel turnaround time and resource utilization rates. The alternative configuration may be particularly advantageous during periods of lower workload, allowing for an agile response to changing demands while maintaining cost efficiency and reducing internal traffic. These findings emphasize the importance of continuous optimization and the application of advanced methodologies in enhancing container terminal operations. The optimized system demonstrates substantial gains in flexibility, especially during varying workload conditions.

Container terminals are complex systems with unknown or highly non-linear relationships that are difficult to model accurately with traditional mathematical techniques. Simulation optimization allows practitioners to model such systems directly and empirically test different scenarios. RSM helps refine these simulations by approximating the response surface and guiding them towards optimal regions. While mathematical models can handle certain types of non-linearity, they are usually more limited by the need for precise mathematical relationships and assumptions (e.g., linearity, continuity). Simulation-based optimization methods make fewer assumptions about the underlying system and are especially useful in real-world applications like container terminal operations, where flexibility, adaptability, and the ability to model uncertainty are critical.

## 4. CONCLUSION

Container terminals play a critical role in the performance of global trade networks, making them a focal point for economic growth and logistical innovations. This paper proposes an RSM approach using a central composite design to develop a metamodel and optimize system configurations at a container terminal that aims to improve operational efficiency. The proposed approach involves several stages for analysis and optimization, demonstrating how RSM can effectively streamline container handling operations. First-order regression models for three critical response variables were developed to explore how different factors influence the system's performance. Then, second-order models were built to capture non-linear relationships between the input factors and responses. Model diagnostic tests provided by analysis of variance (ANOVA) were used to demonstrate the adequacy of the fitted metamodel. Using the Derringer-Suich multi-response optimization procedure, the optimal configuration was identified by considering multiple response variables simultaneously. Implementation results reveal the potential for container terminals to operate more efficiently through careful planning and resource optimization. By optimizing the number of required YTs and cranes, companies can significantly reduce operating costs, which is critical in a competitive global market. Reducing unnecessary equipment can also mitigate congestion within the terminal, enhancing overall productivity and service levels. This study demonstrates the effectiveness of RSM in optimizing handling operations like loading, unloading, and stowage at maritime container terminals. By incorporating automation and optimization techniques, the efficiency of port operations can be greatly improved. Future research could focus on integrating Port 4.0 technologies, the extension of the Industry 4.0 paradigm to the port and maritime industry, with optimization methods to drive innovation in transportation.

## REFERENCES


[1] Guo, H. X.; Ni, S. Q.; He, Y. Y. (2023). Multi-vehicle scheduling of containers in highway port under network condition, *International Journal of Simulation Modelling*, Vol. 22, No. 3, 438-449, doi:10.2507/IJSIMM22-3-652

[2] Grubišić, N.; Dundović, Č.; Žuškin, S. (2016). A split task solution for quay crane scheduling problem in mid-size container terminals, *Technical Gazette*, Vol. 23, No. 6, 1723-1730, doi:10.17559/TV-20150914110215

[3] Goodchild, A. V.; Daganzo, C. F. (2006). Double-cycling strategies for container ships and their effect on ship loading and unloading operations, *Transportation Science*, Vol. 40, No. 4, 473-483, doi:10.1287/trsc.1060.0148

[4] Goodchild, A. V.; Daganzo, C. F. (2007). Crane double cycling in container ports: planning methods and evaluation, *Transportation Research Part B: Methodological*, Vol. 41, No. 8, 875-891, doi:10.1016/j.trb.2007.02.006

[5] Zhang, H.; Kim, K. H. (2009). Maximizing the number of dual-cycle operations of quay cranes in container terminals, *Computers & Industrial Engineering*, Vol. 56, No. 3, 979-992, doi:10.1016/j.cie.2008.09.008

[6] Nguyen, V. D.; Kim, K.-H. (2010). Minimizing empty trips of yard trucks in container terminals by dual cycle operations, *Industrial Engineering and Management Systems*, Vol. 9, No. 1, 28-40, doi:10.7232/iems.2010.9.1.028

[7] Lee, C.-Y.; Liu, M.; Chu, C. (2015). Optimal algorithm for the general quay crane double-cycling problem, *Transportation Science*, Vol. 49, No. 4, 957-967, doi:10.1287/trsc.2014.0563

[8] Zhang, Y.; Rong, Z.; Liu, Z.-X. (2014). The integrated scheduling problem in container terminal with dual-cycle operation, I*nternational Journal of Simulation Modelling*, Vol. 13, No. 3, 335-347, doi:10.2507/IJSIMM13(3)CO12

[9] Wang, D.; Li, X. (2015). Quay crane scheduling with dual cycling, *Engineering Optimization*, Vol. 47, No. 10, 1343-1360, doi:10.1080/0305215X.2014.963070

[10] Zeng, Q.; Diabat, A.; Zhang, Q. (2015). A simulation optimization approach for solving the dual-cycling problem in container terminals, *Maritime Policy & Management*, Vol. 42, No. 8, 806-826, doi:10.1080/03088839.2015.1043362

[11] Zhang, R.; Jin, Z.; Ma, Y.; Luan, W. (2015). Optimization for two-stage double-cycle operations in container terminals, *Computers & Industrial Engineering*, Vol. 83, 316-326, doi:10.1016/j.cie.2015.02.007

[12] Ku, D.; Arthanari, T. S. (2016). On double cycling for container port productivity improvement, *Annals of Operations Research*, Vol. 243, No. 1-2, 55-70, doi:10.1007/s10479-014-1645-z

[13] Chu, Y.; Zhang, X.; Yang, Z. (2017). Multiple quay cranes scheduling for double cycling in container terminals, *Plos One*, Vol. 12, No. 7, Paper e0180370, 19 pages, doi:10.1371/journal.pone.0180370

[14] Zhang, X.; Zeng, Q.; Sheu, J.-B. (2019). Modeling the productivity and stability of a terminal operation system with quay crane double cycling, *Transportation Research Part E: Logistics and Transportation Review*, Vol. 122, 181-197, doi:10.1016/j.tre.2018.12.003

[15] Kamble, S. S.; Gunasekaran, A.; Raut, R. D. (2019). Analysing the implementation barriers of dual cycling in port container terminal using interpretive structural modelling – Indian context, *International Journal of Logistics Research and Applications*, Vol. 22, No. 2, 119-137, doi:10.1080/13675567.2018.1492531

[16] Tang, G.; Qin, M.; Zhao, Z.; Yu, J.; Shen, C. (2020). Performance of peak shaving policies for quay cranes at container terminals with double cycling, *Simulation Modelling Practice and Theory*, Vol. 104, Paper 102129, 16 pages, doi:10.1016/j.simpat.2020.102129

[17] Deniz, E.; Tuncel, G.; Yalcinkaya, O.; Esmer, S. (2021). Simulation of multi-crane single and dual cycling strategies in a container terminal, *International Journal of Simulation Modelling*, Vol. 20, No. 3, 465-476, doi:10.2507/IJSIMM20-3-559

[18] Ahmed, E.; El-Abbasy, M. S.; Zayed, T.; Alfalah, G.; Alkass, S. (2021). Synchronized scheduling model for container terminals using simulated double-cycling strategy, *Computers & Industrial Engineering*, Vol. 154, Paper 107118, 17 pages, doi:10.1016/j.cie.2021.107118

[19] Fontes, D. B. M. M.; Homayouni, S. M. (2023). A bi-objective multi-population biased random key genetic algorithm for joint scheduling quay cranes and speed adjustable vehicles in container terminals, *Flexible Services and Manufacturing Journal*, Vol. 35, No. 1, 241-268, doi:10.1007/s10696-022-09467-6

[20] Cai, L.; Li, W.; Zhou, B.; Li, H.; Yang, Z. (2024). Robust multi-equipment scheduling for U-shaped container terminals concerning double-cycling mode and uncertain operation time with cascade effects, *Transportation Research Part C: Emerging Technologies*, Vol. 158, Paper 104447, 31 pages, doi:10.1016/j.trc.2023.104447

[21] Tan, C.; Qin, T.; He, J.; Wang, Y.; Yu, H. (2024). Yard space allocation of container port based on dual cycle strategy, *Ocean & Coastal Management*, Vol. 247, Paper 106915, 8 pages, doi:10.1016/j.ocecoaman.2023.106915

[22] Li, Y.; Sun, Z.; Hong, S. (2024). An exact algorithm for multiple-equipment integrated scheduling in an automated container terminal using a double-cycling strategy, *Transportation Research Part E: Logistics and Transportation Review*, Vol. 186, Paper 103565, 26 pages, doi:10.1016/j.tre.2024.103565

[23] Myers, R. H.; Montgomery, D. C.; Anderson-Cook, C. M. (2009). *Response Surface Methodology: Process and Product Optimization Using Designed Experiments*, 3rd ed., John Wiley & Sons, Inc., New York

[24] Yu, Y. X.; Huang, Y.; Geng, H. H.; Cha, L. L. (2022). Process parameters optimisation for spring seat based on response surface methodology, *International Journal of Simulation Modelling*, Vol. 21, No. 2, 332-340, doi:10.2507/IJSIMM21-2-CO7